This is the accepted version of the paper. Please cite this paper as:

E. Corti, B. Gotsmann, K. Moselund, I. Stolichnov, A. Ionescu and S. Karg, "Resistive Coupled VO2 Oscillators for Image Recognition," 2018 IEEE International Conference on Rebooting Computing (ICRC), McLean, VA, USA, 2018, pp. 1-7, doi: 10.1109/ICRC.2018.8638626.

Resistive coupled VO_2 oscillators for image recognition

Elisabetta Corti[1,2], Bernd Gotsmann[1], Kirsten Moselund[1], Igor Stolichnov[2], Adrian Ionescu[2], Siegfried Karg[1]

[1] IBM Research – Zurich, Rüschlikon, Switzerland

[2]Nanoelectronic Devices Laboratory, École Polytechnique Fédérale de Lausanne, Lausanne, Switzerland

***Abstract*—Oscillator networks are known for their interesting collective behavior such as frequency locking, phase locking, and synchronization. Compared to other artificial neural network implementations, timing rather than amplitude information is used for computation. We have fabricated and simulated small networks of coupled VO_2 oscillators and investigated the electrical behavior. It is demonstrated experimentally and through simulations that the coupled oscillators lock in frequency and the phase relation can be adjusted by the coupling resistance. Pattern recognition was simulated in resistor-coupled networks with up to nine oscillators (pixels), demonstrating the possibility of implementation of this task with compact VO_2 circuits.**

Keywords—neural network; oscillating; phase; timing; resistor-coupled; pattern recognition

I. INTRODUCTION

Brain-inspired computing has gained increasing interest in the last few years. Conventional computing systems based on Von Neumann architecture have proven to be inefficient when solving complex problems involving for example unstructured data classification and pattern recognition [1,2]. In comparison, human brain is highly efficient in dealing with these tasks, leading to the conclusion that an alternative architecture based on neurological models has the potential of increased computational power for low-energy, fault-tolerant computations [3]. Moreover, algorithms for machine learning and neural networks suffer from Von Neumann bottleneck problem, being slowed down by the many access to the memory that the system has to perform. The realization of alternative, non-Boolean architectures can offer a solution to this problem [4].

In this frame, physical phenomena as the synchronization of dynamical systems, that are ubiquitous in nature, are being explored as the base for neural networks architectures [5,6]. In particular, it has been demonstrated that networks of weakly coupled oscillators can be used to implement pattern recognition or to solve the 10-city salesman problem [7,8]. Weakly coupled oscillators have the property to lock in frequency, while maintaining a fixed phase difference, that is determined by the weight of the coupling. Changing the coupling strength, the phase relation between the oscillators can be tuned, advancing the possibility of encoding information in the phase relation.

Very compact relaxation oscillators have been recently fabricated exploiting the phase change properties of VO_2 [9] and implementing simple electrical connections, opening the possibility of realization of highly scalable, fully connected oscillator networks can be realized [10,11].

In this conceptual study we show the first demonstration on how resistive-coupled VO_2 oscillators can be used for neuromorphic computing applications, more specifically for pattern recognition.

Compared to previous works, that obtained stable phase relations only in capacitive coupled oscillators [11,12] we show through experimental results that it is possible to couple oscillators with resistive components. In this paper in-phase and out-of-phase oscillation are achieved experimentally and through matching simulation, tuning the coupling resistance in a system of two-coupled oscillators. These results offer the prospective of implementation of the coupling with phase-change memories or resistive RAM [13], that not only is relevant for integration with novel CMOS compatible technologies but would also allow to apply machine learning techniques by having an electrically tunable coupling. Further, encoding the relevant information in the phase of the signal rather than the amplitude provides a higher noise robustness in highly scaled voltage technologies.

In Section IV, mathematical simulations of a system of nine coupled oscillators are performed, proving that pattern recognition can be implemented with the given network. Results of successful recognition of an image in less than 10 oscillating cycles are shown. The perspective is to employ small, layered and fast networks of oscillators as filters in convolutional neural networks.

II. CIRCUIT SIMULATION AND EXPERIMENTAL PROCEDURES

In this section, we present the electrical model used to perform circuit simulation on VO_2 coupled oscillators (part A). Details on the device fabrication and the experimental setup are given in parts B and C.

A. Circuit simulations

The dynamical behavior of the oscillating circuits is studied using the electronic simulation package Cadence Virtuoso 6.1.6. The hysteretic behavior of the phase-change of VO_2 was

tackled by a driving point equivalent circuit with abrupt transition [14]. The circuit model makes use of a comparator to determine the state – high or low impedance – of the VO_2 resistor. The information is stored in the capacitor C, and the voltage of the capacitor is used to drive a switch that determines the impedance at the input pins of the model (Figure 1a). The system is duplicated to make it bipolar.

Linear and semi-logarithmic representations of a simulated I-V characteristic are shown in Figure 1b and 1c, respectively. The steepness of the metal to insulator transition is determined by the slew rate of the operational amplifier and limited by the time constant $\tau_0=C\times R$ of the output circuit. The voltage thresholds for the transition to high and low impedance state are directly modelled by the VCVS (voltage controlled voltage source) with the relation:

$$V^+=V_{TL}+(V_{TH}-V_{TL})\times Vo.$$

B. Device fabrication

The VO_2 switches were fabricated on oxidized 4" silicon wafers (thickness SiO_2: 1µm). A 45 nm-thick VO_2 layer was deposited with pulsed laser-deposition and patterned using electron-beam lithography and ICP etching. Electrical contacts were provided through thermal evaporation of nickel (100nm) and gold (20nm) and lift-off technique. Figure 2 shows a typical device consisting of two metal leads contacting a polycrystalline VO_2 stripe. The dimensions of the gap between the electrodes

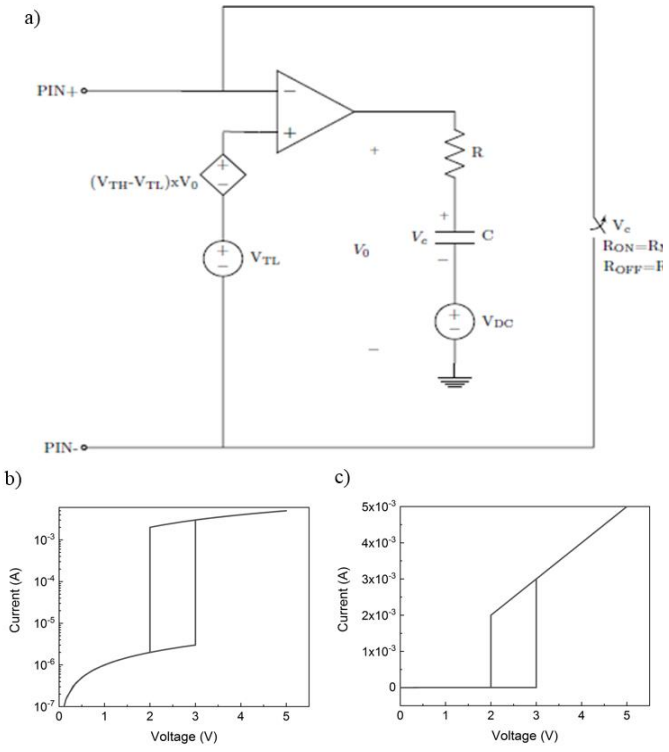

Figure 1: a) equivalent circuit model of the VO_2 resistor and the resulting I-V characteristic, in b) logarithmic and c) linear scale.

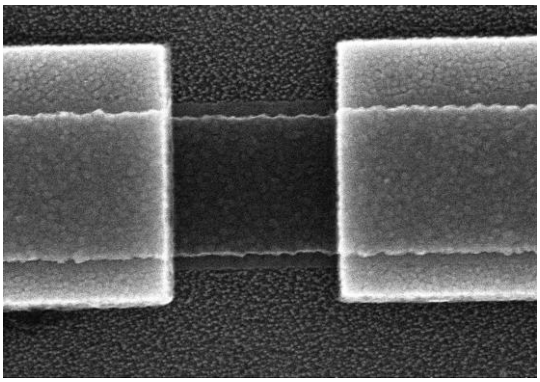

Figure 2: SEM image of a fabricated device consisting of a VO_2 stripe contacted by two metal electrodes (Ni/Au bilayer). Dimensions: width VO_2 stripe: 700nm, thickness VO_2: 45nm, contact separation 900nm.

and the width of the stripe were varied from 100 nm to several micrometer. The granularity of the VO_2 layer limits currently further downscaling. However, further optimization of the material deposition is in progress. The ultimate limit in scalability will depend on the stability of the crystal phases in devices consisting of only few lattice cells. Figure 3b shows the measurement of the hysteresis cycle of devices for different widths of the VO_2 stripes. The resistance was measured over a temperature sweep from 295 to 355K. The transition from the insulating to the metallic state happens around 340K. Due to deposition on amorphous substrate, the VO2 layer is polycrystalline, impacting on the hysteresis that widens to 15K width [15].

C. Measurement setup

The basic relaxation oscillator consists of a switching VO_2 resistor R_V, a parallel capacitor C_P and a serial load resistor R_S (see Figure 3a). An applied d.c. voltage is charging the capacitor C_P and leads to Joule heating of the semi-insulating VO_2 resistor R_V. When the temperature in the VO_2 resistor exceeds 340K the resistivity of VO_2 decreases by 2 to 3 orders of magnitude. The

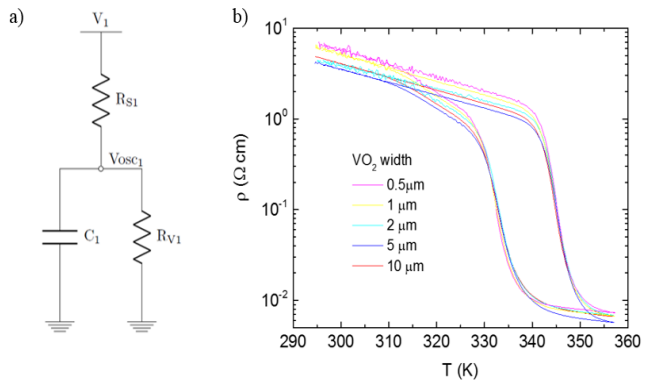

Figure 3: a) basic oscillator circuit scheme
b) resistivity of 10 µm-long VO_2 stripes with different width vs. temperature at phase-transition

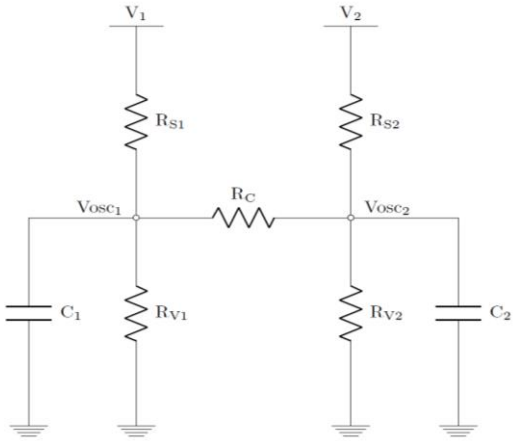

Figure 4: Circuit scheme of two resistor-coupled VO_2 oscillators

lower R_V discharges the capacitor and the voltage at V_{osc1} drops. Hence, Joule heating is reduced and the VO_2 temperature decreases, which causes again a phase-change in the material and a metal-insulator transition. The VO_2 resistance increases and the cycle starts again.

The Si chips with the VO_2 resistors were measured in vacuum using a temperature-controlled probe-station. External contacts to 8 individual VO_2 devices were provided by a 16-pin probecard and combined to oscillating circuits using discrete external capacitors and resistors. Time-resolved measurements were performed with a multi-channel data acquisition (National Instruments) system which includes programmable resistor modules implementing variable series and coupling resistances.

For all the measurements the value of the capacitor was chosen to be C_P=150nF, large enough to make all the measurement independent from parasitic effects. Moreover, this value determines the time constant of the circuit, that was deliberately made quite slow not to hit the timing resolution boundaries of the instrumentation.

III. TWO RESISTIVE-COUPLED VO_2 OSCILLATORS: EXPERIMENTS AND SIMULATIONS

In this section we show experimentally resistive-coupled VO_2 oscillators and matching electrical simulation. After the chips were mounted in the cryostat, the chip temperature was kept at a constant value of 320K during the measurements. Two VO_2 switches with equal dimensions were contacted and values for the input voltages V_1 and V_2 as well as for the series resistances R_{S1} and R_{S2} were chosen to establish stable oscillation conditions for the individual VO_2 oscillators. Then, the oscillators were connected to each other in the circuit configuration shown in Figure 4 with a programmable resistor R_C.

The spontaneous oscillations of two coupled VO_2 resonators are shown in Figure 5. An input voltage of 3.2 V was applied to both oscillators. Setting a coupling resistors R_C = 3kΩ leads to in-phase coupling of the oscillators whereas R_C=9kΩ couples

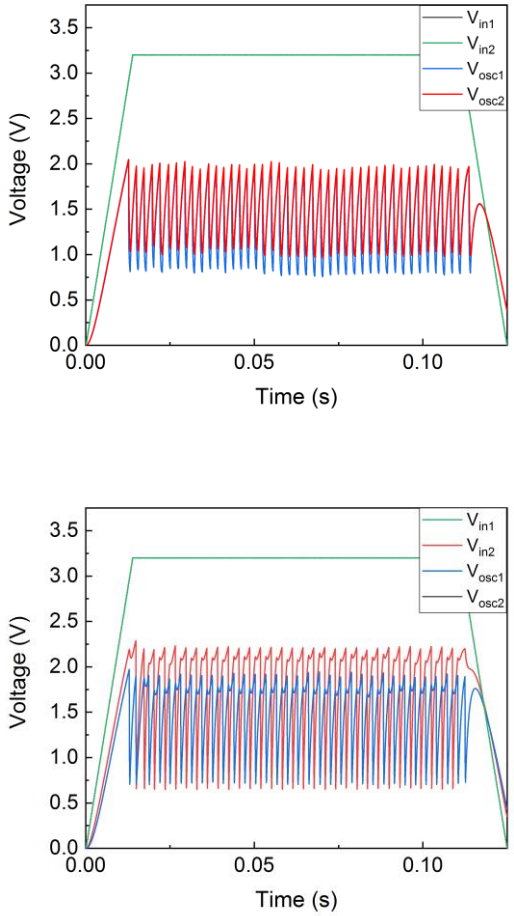

Figure 5: Measured voltage oscillations of coupled VO_2 resonators. R_C=3kΩ results in in-phase coupling (top), R_C=9kΩ in out of phase coupling (bottom). V_1=V_2=3.2V, R_{S1}=26 kΩ, R_{S2}=12 kΩ, C_1=C_2=150nF.

them out-of-phase. The frequencies are 420 Hz for in-phase and 312 Hz for out-of-phase coupling. The phase difference between the signals of the two oscillators was measured, resulting in $\Delta\varphi$=1.06° for the in-phase coupling and $\Delta\varphi$=179° for the out-of-phase coupling. Although the physical dimensions of the two VO_2 switches are the same, the threshold voltages of the two oscillators differ by several hundred mV. We attribute this to the granular nature of the VO_2 layers.

Using the parameters obtained in **Error! Reference source not found.**5, we simulated the coupled circuit (see Figure 6) using the model from II.A. The threshold voltages considered are the ones measured from Fig. 5: V_{TH1}=1.9V, V_{TL1}=0.77V, V_{TH2}=2.2V, V_{TL2}=0.67V for out-of-phase configuration and V_{TH1}=2V, V_{TL1}=0.77V, V_{TH2}=2.1V, V_{TL2}=1V for in-phase coupling. For determining the values of the metallic and insulating state resistances, the current of one oscillator was evaluated as: $I_{osc1}=(V_1-V_{osc1})/R_{s1}-(V_{osc1}-V_{osc2})/R_c$. From the relation: $Z_1=V_{osc1}/I_{osc1}$ the impedance of the oscillator was evaluated at each time. Since this measurement comprehends the current coming from the capacitor, this equivalent impedance

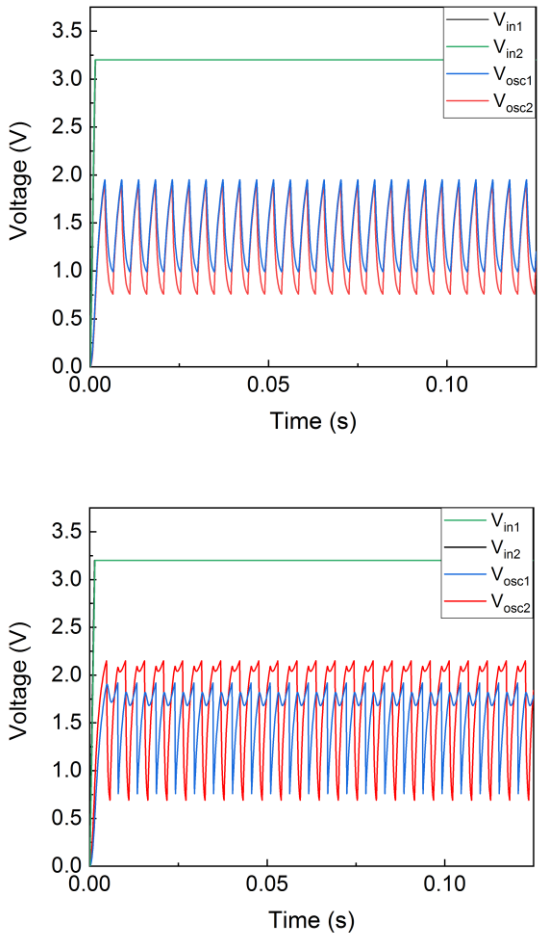

Figure 6: Simulated voltage oscillations of coupled VO_2 resonators with parameters given in Figure 5.

can give only an indication of the value of the resistance of the VO_2 stripes for the insulating and metallic phase. Therefore, the values of resistances in the insulating and metallic states were tuned in the simulation in order to reproduce the behavior of the experimental results. The final values used in the simulation are R_{V1H}=39.4kΩ and R_{V2H}=23kΩ for the high impedance state and R_{V1L}=7.6kΩ, R_{V2L}=2.8kΩ for the low impedance state. Simulated and measured oscillations show similar features and almost equal oscillating frequencies. The phase difference between the two oscillators in the in-phase and the out-of-phase state in the simulations are constant over time, since the variability in the switching threshold that is present in the experiment wasn't considered. In the out-of-phase case, both in simulation and experiment, the oscillations present a double peak shape. This is attributed to the fact that the coupling resistance used is rather small (9kΩ): as one of the oscillators changes from the metallic to the insulating state, the equivalent impedance seen from the other oscillator changes accordingly, and the voltage partition between the series resistance and the equivalent resistance causes the double peak behavior. Increasing the coupling resistance, the equivalent resistance is seen from the first oscillator towards the other is less sensitive to variation of the impedance of the second oscillator, and the double peak can therefore be suppressed.

In a network of two coupled oscillators only 2 stable phase conditions exist. As validated with systematic electrical simulations scanning the coupling-resistance parameter space, every intermediate phase relation is converging within 2-3 oscillations to either in-phase or out-of-phase coupling.

Although the VO_2 resistors exhibit different impedance and threshold values, they are still able to lock to the same frequency and their phase can be tuned with the coupling strength. However, the larger the mismatch the narrower the window for tuning the phases becomes. In this example, the in-phase configuration is less stable, and small deviations lead to a shift into the out-of-phase configuration. The electrical simulations validate this result and further predict higher stability for the in-phase coupling in case of VO_2 resistors with identical characteristics.

The variability of the sample impedances makes experiments of coupling more than two oscillators currently difficult. It is noted that the variability of the device is given by the granularity of the VO_2 stripes. Processing improvements of the material are in progress. An ultimate solution would be to use single crystalline VO_2, that can be obtained by deposition on crystalline TiO_2 substrates: this would allow to obtain high uniformity throughout the devices and overall better performances (R_{on}/R_{off} ratio can be improved [15]). The disadvantage of this solution would be the loss of CMOS process compatibility, and therefore exploration of wafer-bonding techniques, similarly to what is done for III-V material, would be needed to retrieve it [16].

IV. Simulation of Pattern Recognition

In this section we present numerical simulations of a network of 9 resistor-coupled oscillators to investigate the capabilities of VO_2 resonators for pattern recognition. We calculated numerical solutions of the basic differential equations using the MATHEMATICA computing system. The phase-transition of VO_2 was approximated using:

$$G_{VO2}(V) = \left[(G_{met} - G_{ins})\left(1 - \frac{1}{1+e^{(V+\mu)/kT}}\right) + G_{ins}\right](1+V^2) \qquad (1)$$

for the voltage dependent conduction with constant values for the metallic and insulating phases of G_{met}=1/1kΩ and G_{ins}=1/1MΩ, respectively. T was set to 10K and μ=(0.5±0.1)V depending on the direction of the voltage change. Figure 7 shows simulated IV and resistance characteristics.

We calculated the temporal dependence of fully connected oscillator networks with nine oscillators. Figure 8 shows an example of a smaller network with 4 fully connected oscillators, where each oscillator is coupled to all other others with a resistor. We will adjust these resistors to obtain desired phase relations of the oscillators which will be the computational output of this network.

In this example, we want the network to memorize three different patterns consisting of 9 black and white pixels (see

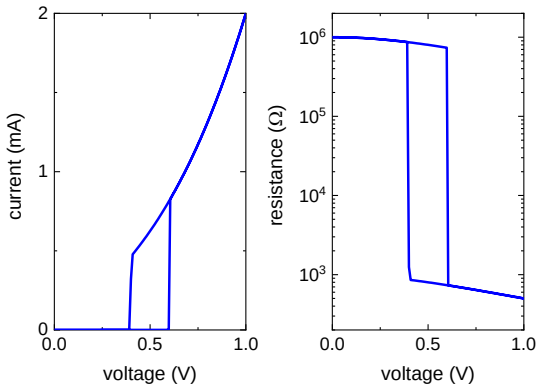

Figure 7: Simulated IV and resistance characteristics

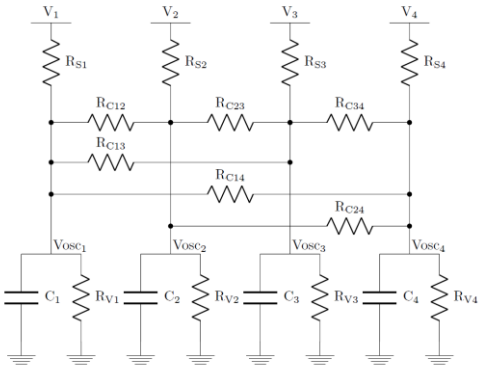

Figure 8: Fully connected network of 4 oscillators

Figure 9 a-c). It will be assumed that white and black pixels are represented by in-phase and out-of-phase oscillations, respectively. The network should be capable to maintain at least 3 different, stable oscillation states. When a search pattern is supplied to the inputs, e.g. pattern d in Figure 9, then network should stabilize in one of the 3 memorized patterns.

The Hebbian learning rule [7], with ϑ^k being the vectors to be memorized:

$$C_{ij} = \frac{1}{n}\sum_{k=0}^{m} \vartheta_i^k \, \overline{\vartheta_i^k}$$

was used to calculate the connection matrix associated with the 3 training patterns resulting in

$$C_{ij} = \frac{1}{18}\begin{pmatrix} \mathbf{1} & \mathbf{1} & \mathbf{1} & 0 & 0 & 0 & 0 & 0 & 0 \\ - & \mathbf{1} & \mathbf{1} & 0 & 0 & 0 & 0 & 0 & 0 \\ - & - & \mathbf{1} & 0 & 0 & 0 & 0 & 0 & 0 \\ - & - & - & \mathbf{1} & \mathbf{1} & \mathbf{1} & 0 & 0 & 0 \\ - & - & - & - & \mathbf{1} & \mathbf{1} & 0 & 0 & 0 \\ - & - & - & - & - & \mathbf{1} & 0 & 0 & 0 \\ - & - & - & - & - & - & \mathbf{1} & \mathbf{1} & \mathbf{1} \\ - & - & - & - & - & - & - & \mathbf{1} & \mathbf{1} \\ - & - & - & - & - & - & - & - & \mathbf{1} \end{pmatrix}$$

We associate the elements on the diagonal with the (invers) series resistances R_{Si} and the off-diagonal elements with the (invers) coupling resistances R_{Cij} and will use a value of 10 kΩ for the non-zero elements in the following simulations. Moreover, for the metallic and semiconducting resistances 1kΩ and 1MΩ were assumed, respectively. For all capacitors a value of 150nF was chosen.

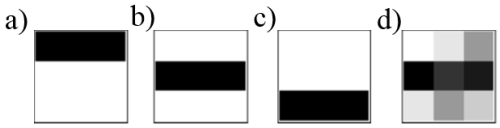

Figure 9: a) – c) training patterns to be memorized by the network, d) search pattern

The network starts oscillating when a d.c. voltage (V_{in} = 1 V) is applied to the inputs. We encode the grey-scale level of the input pattern using a delayed application of the input voltage. For a white pixel, the input is triggered at time 0 whereas a black pixel is triggered with a time delay τ_D and any grey pixel with a proportional fraction of τ_D (see Figure 10).

Figure 11 shows the simulated voltage pattern of the 9 oscillators, when channels 4-6 are triggered with a delay τ_D = 210 µs after the other channels (correlating to training pattern b in Figure 8). After some initiation phase, all channels oscillate with a stable period of 666 µs and the voltage drop across the VO_2 oscillators varies between 0.4 V and 0.6 V. The phase shift of the 'black' pixels (oscillators 4-6) stabilizes at ~220 µs with respect to the 'white' pixels (oscillators 1-3 and 7-9), i.e. a phase difference of ~⅔π is maintained. Similar results are obtained when the first or last 3 channels are delayed (corresponding to patterns a and c in Figure 9). Figure 12 shows the voltage oscillations of the network when the search pattern from figure 9d is applied. The input voltage of the 9 channels is triggered a different delay times corresponding to the grey-scale of the search pattern.

After 4 – 5 oscillations, again, a stable pattern establishes with the same constant period of 666 µs. The phases of the 'black' and 'white' pixel is shifted by ~150 µs. The phase differences for the 9 oscillators are determined at the oscillation peaks and plotted against the peak number in Figure 13 for the training pattern (a) and the search pattern (b). The delay used for the input pattern is included as peak position 0 for illustration. Moreover, input and output patterns are displayed as grey-scale

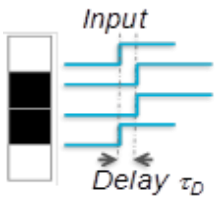

Figure 10: The network input is delay-time encoded application of the voltage to each channel. For a white pixel, the input is triggered at time 0, a black pixel is triggered with a time delay τ_D and any grey pixel with a proportional fraction of τ_D.

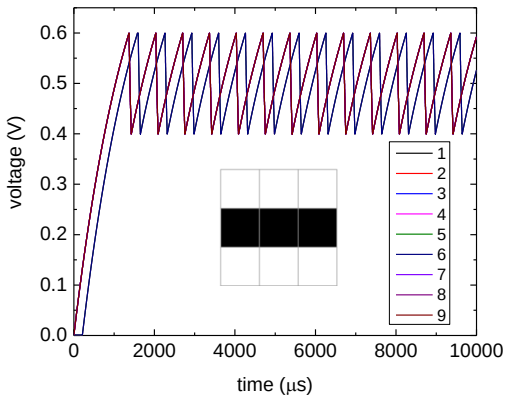

Figure 11: Simulated voltage pattern of 9 oscillators. Input channels 4-6 are triggered with a delay of τ_D = 210 µs after the other channels (correlating to training pattern b in figure 8). Traces of delayed and undelayed channels fall on top of each other, respectively.

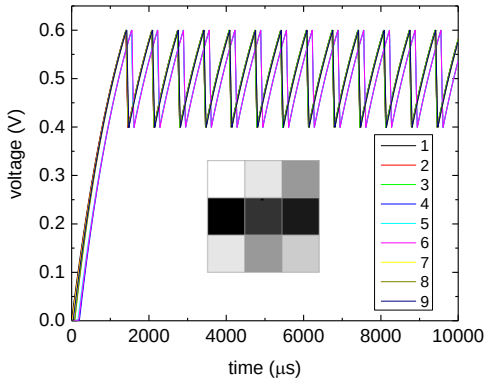

Figure 12: Simulated voltage pattern using the gray-scale test pattern (Figure 9d) as input, i.e. channels are started with different delay times.

images in the inset. Although the phase differences of the search patterns are smaller than in the case of the memorized pattern, the network clearly 'classifies' the search pattern as one of the training patterns.

Variability in the components was taken into account in the simulations, both in the VO_2 switching threshold values and in the metallic and insulating resistances. Results show that the image recognition is successful even with component variability as long as the mismatch is less than 10%.

This simulation demonstrates that it is possible to perform pattern recognition with the given network. Scalability to larger images is currently under study, and could in principle be performed limiting the coupling of a single oscillator to the neighbouring ones. Aiming for application in convolutional neural networks (CNNs), the target size for coupled oscillator network is a 7x7 or 11x11 array, that is the standard for filtering feature extractors in multi-layered networks [17, 18]. The 3x3

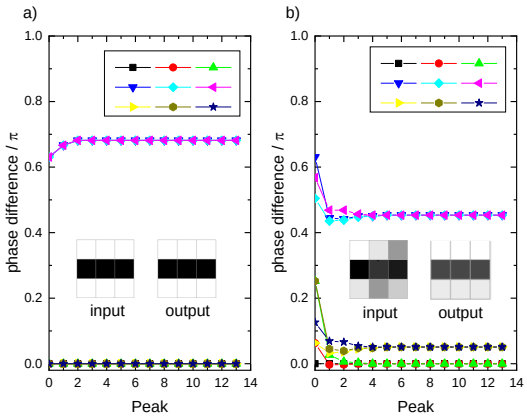

Figure 13: Phase differences determined at the peak positions from figures 11 and 12 for the training pattern (a) and the search pattern (b), respectively. Peak position 0 indicates the input delay. Grey-scale images in the inset display input and output patterns.

oscillator matrix presented is a demonstrator for a first layer of a CNNs. Multiple layers can be stacked feeding one or more outputs of one layer into the input of the next layer using non-linear electrical devices [19].

For practical implementation in modern computer architectures, it is necessary to encode and decode the phase information at the input and output of the neural network. The perspective is to use time-to-digital converters (TDC), a technology that is an industrial standard for PLLs [20], to perform this task.

V. Conclusions

With VO_2 metal-insulator switches highly scalable electrical oscillators can be built. This enables to fabricate oscillating networks with much smaller footprint than other implementations, for instance, phase-locked loop, MEMS or optical resonators. Compared to other artificial neural network implementations, timing rather than amplitude information is used for computation which has several advantages in terms of noise reduction. The time delay of the input voltage is used as input signal and phase information of oscillation as output signal.

We showed for the first time through experimental results and circuits simulations that control of phase is possible with resistors as coupling elements. With two oscillators stable in-phase and out-of-phase coupling has been demonstrated. Simulations of larger networks reveal that simple pattern recognition can be performed with resistor-coupled oscillators, opening the perspective of employing this technology for dedicated hardware for convolutional neural networks. Memorized patterns correspond to stable phase correlations of the oscillators. When an unknown search patterns is provided at the inputs the network will relax to the closest stable configuration within a few oscillation periods and output the corresponding memorized pattern.

ACKNOWLEDGMENT

This work has been supported by the HORIZON2020 PHASE-CHANGE SWITCH Project (Grant. No. 737109).

REFERENCES

[1] C. D. Schuman *et al.*, "A Survey of Neuromorphic Computing and Neural Networks in Hardware," [online] CoRR, abs/1705.06963, 2017.

[2] J. Misra and I. Saha, "Artificial neural networks in hardware: A survey of two decades of progress," *Neurocomputing*, vol. 74, no. 1–3, pp. 239–255, 2010.

[3] D. Kuzum, S. Yu, and H. S. Philip Wong, "Synaptic electronics: Materials, devices and applications," *Nanotechnology*, vol. 24, no. 38, 2013.

[4] G. Indiveri and S. C. Liu, "Memory and Information Processing in Neuromorphic Systems," *Proc. IEEE*, vol. 103, no. 8, pp. 1379–1397, 2015.

[5] M. J. Cotter, Y. Fang, S. P. Levitan, D. M. Chiarulli and V. Narayanan, "Computational Architectures Based on Coupled Oscillators," *2014 IEEE Computer Society Annual Symposium on VLSI*, Tampa, FL, 2014, pp. 130-135.

[6] F. Y. Shih, "Pattern Recognition," *Image Process. Pattern Recognit.*, vol. 62, no. 6, pp. 306–352, 2010.

[7] Izhikevich, "Computing with Oscillators," *Neural Networks*, no. 5255, pp. 1–30, 2000.

[8] Endo, T. and Takeyama, K. (1992), "Neural network using oscillators," Electron. Comm. Jpn. Pt. III, 75: 51-59.

[9] H. T. Kim et al., "Mechanism and observation of Mott transition in VO2 based two- and three- terminal devices," *New J. Phys* vol. 6, pp. 52-52, 2004.

[10] N. Shukla et al., "Synchronized charge oscillations in correlated electron systems", *Sci. Rep.* 4, doi:10.1038/srep04964 (2014).

[11] A. Parihar, N. Shukla, S. Datta, and A. Raychowdhury, "Synchronization of pairwise-coupled, identical, relaxation oscillators based on metal-insulator phase transition devices: A model study," *J. Appl. Phys.*, vol. 117, no. 5, 2015.

[12] V. V Perminov, V. V Putrolaynen, M. A. Belyaev, and A. A. Velichko, "Synchronization in the system of coupled oscillators based on VO 2 switches," *J. Phys. Conf. Ser.*, vol. 929, no. 1, pp. 12045, 2017

[13] G. W. Burr et al. "Neuromorphic computing using non-volatile memory," *Advances in Physics: X*, vol. 2, no. 1, pp. 89-124, 2016.

[14] P. Maffezzoni, L. Daniel, N. Shukla, S. Datta, and A. Raychowdhury, "Modeling and Simulation of Vanadium Dioxide Relaxation Oscillators," *IEEE Trans. Circuits Syst. I Regul. Pap.*, vol. 62, no. 9, pp. 2207–2215, 2015.

[15] A. Pergament, G. Stefanovich, and A. Velichko, "Oxide Electronics and Vanadium Dioxide Perspective: A Review," *J. Sel. Top. Nano Electron. Comput.*, vol. 1, no. 1, pp. 24–43, 2013.

[16] L. Czornomaz *et al.*, "An integration path for gate-first UTB III-V-on-insulator MOSFETs with silicon, using direct wafer bonding and donor wafer recycling," *2012 International Electron Devices Meeting*, San Francisco, CA, 2012, pp. 23.4.1-23.4.4.

[17] Krizhevsky et al., "ImageNet Classification with Deep Convolutional Neural Networks". Neural Information Processing Systems, n 25, vol 1.

[18] P. Sermanet, D. Eigen, X. Zhang, M. Mathieu, R. Fergus, and Y. LeCun. "Overfeat: Integrated recognition, localization and detection using convolutional networks". CoRR, abs/1312.6229, 2013.

[19] S. Karg, B. Gotsmann, F. Menges, "Multi-layer oscillating network", patent submitted.

[20] R. B. Staszewski, S. Vemulapalli, P. Vallur, J. Wallberg and P. T. Balsara, "1.3 V 20ps time-to-digital convrter for frequency synthesis in 90-nm CMOS," *IEEE Trans. On Circuit ans Systems II*, vol. 53, no. 3 , pp. 220-224, 2006.